Gamma-Probe for Locating the Source of Ionizing Radiation

Jake Hecla, Timur Khabibullin, Anastasia Tolstaya

National Research Nuclear University "MEPhI" (Moscow Engineering Physics Institute)
Kashirskoe highway 31, 115409, Moscow, Russian Federation
Massachusetts Institute of Technology, Cambridge, United States
tolstaya.a@inbox.ru

Abstract
The radionuclide diagnostics unit, described in the article, detects pathological changes of organs and systems of a person. The device is a portable detector of gamma rays that allows to diagnose superficial malignancies using radiopharmaceuticals injected into the body. The gamma probe uses crystal LaBr3:Ce as a scintillator and silicon photomultiplier SiPM as a photodetector. The focus of this paper is the improvement of the amplifier, which originally produced misshapen pulses unsuitable for energy discrimination. Using LTSPICE, a free circuit-modelling program, we performed extensive simulation of both the SiPM and the amplifier. From this work, we determined that high input impedance and unnecessarily high gain were the source of the distortion. Another amplifier better suited to the SiPM parameters was simulated and then prototyped.

Keywords: Gamma-Probe, Cancer Detection, Lymph Nodes, Detector Resolution, SiPM, Amplifier, Collimator

1 Introduction

Cancer is a generic term for a large group of diseases that can affect any part of the body. Other terms used for that group are malignant tumours and neoplasms. A characteristic feature of cancer is rapid creation of abnormal cells that grow beyond their usual boundaries, and which can invade adjoining parts of the body and spread to other organs. This process is called metastasis. Metastases are the major cause of death from cancer. (Blokhin and Blokhin 1979, Cancer. Fact sheet N°297 2015)

Cancer is a major cause of morbidity and mortality all over the world: in 2012, 14 million new cases were detected and 8.2 million deaths associated with cancer occurred. According to forecasts, the number of cases of cancer will continue to grow from 14 million to 22 million over the next two decades (De Martel et al. 2012, IARC Nonserial Publication, 2014).

According to the World Health Organization, more than 30% of cancer deaths can be prevented by avoiding or changing the main risk factors, which include: tobacco use, overweight or obesity, eating insufficient amounts of fruit and vegetables, physical inactivity, alcohol consumption, ionizing and non-ionizing radiation (Cancer. Fact sheet N°297 2015).

Nuclear medicine is an independent branch of beam diagnostics and radiology aimed at, in particular, recognizing pathological changes of organs and systems of a person using radiopharmaceuticals (RPh). RPh is a chemical compound, which contains a specific radionuclide in its molecule. Usually short-lived radionuclides of technetium are used. In clinical practice, the following types of radionuclide investigations are implemented: visualization of organs, i.e. getting their radionuclide imaging; measuring the accumulation of radiopharmaceuticals in the body and their elimination; measuring the radioactivity of samples of biological fluids and tissues of the human body and in vitro tests. RPh are able to selectively accumulate in organs and tissues affected by malignant neoplasms, which is what happens after a certain period of time characteristic of this RPh. The radiation emitted by a radioactive isotope, which is part of the RPh can be registered by means of a special device: the count rate of gamma rays will be maximum at the location of the tumour. Thus, it is possible to diagnose the tumour and its location in the body, which is defined as an area of increased concentration of RPh. (Zubovsky G.A. 1978, Clinical Radiology 1985).

Diagnostic instruments used in nuclear medicine, usually include a detector, a scanner, a converter unit and a memory block. A special type of such devices are compact gamma-probes designed to identify areas of local accumulation of the radiopharmaceuticals in the body. (Gamma Probes 2014, Da Costa et al. 2005, Wengenmair and Kopp 2005)

Main applications of gamma-probes are intraoperative search for sentinel lymph nodes and non-invasive body scan of patients to detect superficial malignancies. (Wei et al. 2015, Romanova 2013, Endo et al. 2014, Matheoud et al. 2014)

The first method is implemented in the following way: the patient is preoperatively administered with a radiopharmaceutical that accumulates in the hearth of a malignant neoplasm (tumour), and in the network of nearby lymph nodes affected by metastases. The surgeon removes the tumour and then extracts the lymph nodes, which are scanned for the presence of metastases one by one with the gamma probe. Since the network of lymph nodes in the body is a diverging network, their consequent check for metastasis is a valid criterion for the spread of metastasis in the body. This procedure can reduce the invasiveness of tumour removal procedures and save the greatest number of healthy tissue of the patient without the risk of relapse.

The second method is completely non-invasive and is an addition to the traditional radionuclide procedures. In some cases (surface location of the tumour or its small diameter) using single-photon or positron emission tomography of the whole body is irrational, since the cost of a procedure is high, but due to the limited number of scanners in the medical centres of the Russian Federation and their bandwidth is small (Bogliolo et al. 2015). In such cases, the rational solution is to conduct local radio diagnostic procedures in the vicinity of the area of the tumour, which comprises administering of RPh to a patient and subsequent scanning of the surface of malignancy location zones using a portable gamma-ray detector.

The gamma-probe is a device aimed to locate gamma emitters intraoperatively. Several devices currently exist on the market for these purposes.(Grigorenko 2015, Lebedev 2016).

For example, a device called a surgical gamma-probe with TlBr semiconductor for identification of sentinel lymph node is quite known, as described in (Da Costa et al. 2005). This surgical gamma-probe uses a crystal TlBr as a scintillator.

The disadvantages of this device are the need for surgical intervention, lack of precision, sensitivity to magnetic fields, lack of immunity to noise of a photomultiplier, small light output of the scintillation crystal and dependence of counting rate from the temperature.

Another device is described in the article by Georgiou (2011). This gamma-probe is based on R8900U-00-C12 position-sensitive photomultipliers coupled to the scintillator, which uses CsI (T1)

crystal, and a general-purpose parallel collimator. The disadvantages of the device are small light output of the scintillation crystal, sensitivity to magnetic fields, and the counting rate dependence on the temperature.

In most cases, a gamma-probe is the main station with an indicator of the radiation intensity and a probe recording gamma rays, which is connected with the station through a wire. The absence of an indicator of radiation intensity on the probe itself is forcing surgeons to often switch their attention from the sensing zone to the display at the main station. This practice not only slows down and complicates the process of tumour search, but also can lead to a loss of the zone of an already detected tumour in the event of external distractions and it can also lead to repeating of the search procedure.

Given the shortcomings of existing devices, it was decided to develop a gamma-probe. The gamma-probe has features that significantly improve on the state of the art through the use of SiPM technology developed at the National Research Nuclear University "MEPhI" (NRNU MEPhI), Russia.

The article discusses two versions of the gamma-probe: Mk. I and Mk. II.

2 Gamma-probe prototype

In general, the developed gamma-probe consists of the following components:

Collimator. It serves to reduce the angle of gamma rays fixing. It is a metal construction – usually a cylinder with a hole. The main area of improvement – the construction itself, its shape and the shape of the hole. Developments in this area are little, and there is no obvious way to achieve a sharp qualitative leap.

Scintillator. It is the main component of the detector. The material, of which it is composed, emits light when capturing gamma rays; the intensity of flashes is directly proportional to the intensity of gamma radiation. The gamma-probes commonly use scintillators LYSO, $Lu_{1.8}Y_{0.2}SiO_5$:Ce), Cadmium Zinc Telluride (CdZnTe), Cadmium Telluride (CdTe), which have the described qualities, but the search for new materials is time consuming and does not give fast efficiency growth.

Silicon photomultiplier. It is a matrix of avalanche photodiodes. It allows detecting and amplifying a weak flash of light intensity (at the level of single photons) and having the duration of the order of ones-hundreds of nanoseconds. The ability to recognize the weakest flash defines the accuracy of the boundaries determination of the cancerous tumour, and specialists keep working on the improvement of these qualities. The development of photomultipliers goes towards increasing the number of diodes and reducing the size of the entire matrix. It depends on the size of technology process, and progress in this area is related to the general miniaturization of electronics. Thus, there are new photomultipliers, more sensitive than those used in common gamma-probes. The new photomultipliers are supposed to improve overall efficiency.

Microcontroller. It is a chip responsible for the processing and interpretation of the signals. The element base used in the current generation of gamma-probes is not only outdated, but also requires a lot of production costs, since the period of support of microcontrollers used in the production already ended or will end soon. In most cases, three generations of microcontrollers have already changed since the last solution development. Using the latest developments in this area will not only add functionality and improve usability, but it will also reduce production costs.

An example of a specific implementation of the proposed device in a general form is shown in Figure 1 and comprises: a detecting element (1) placed in the collimator (2), an amplifier (3), a comparator (4), a logic analyser FPGA (field-programmable gate array – circuit logic elements in the programmable operating conditions) (5), data interface (6), a digital-to-analogue converter (DAC) (7), the SPI (Serial Peripheral Interface) bus (8), the power supply circuit (9) and the connection circuit (10). The connection circuit is connected to the switching power supply circuit, which in its turn is connected to each element of the system via the SPI bus.

The detection element is placed in the collimator and consists of a $LaBr_3$:Ce crystal and a silicon photomultiplier SiPM which is used as a photomultiplier tube. Protection from scattered radiation and background activity surrounds the detecting part at sides and forms a narrow field of view of the detector to improve the ratio "signal – noise".

$LaBr_3$:Ce crystal was selected as a scintillator due to its following features:

- high detection efficiency (efficiency level of NaI detection);
- non-hygroscopicity of the scintillator, i.e. the possibility to work with it in the open air without additional protection from moisture for the crystal;
- high value of effective atomic number;
- short decay time.

SiPM was selected as the photodetector of the gamma-probe selected due to its following features:

- the operating voltage is approximately 2V higher than U_{break} (breakdown voltage) and U_{break} is only tens of Volts;
- an excellent signal/noise ratio (SNR) compared to conventional avalanche photodiode;
- no damage from excessive light;
- durable (rugged) and stable;
- minimum requirements for electronics;
- small spread gain (less than 10%);
- low sensitivity gain to changes in temperature and voltage supply (to temperature change ~3% 10°C, to change of the voltage bias of ~1% per 30mV);
- the possibility of registering nanosecond flashes of light without distortion of detected pulse form;
- the ability to work both in the pulse counting mode, and in spectrometric mode;
- good time resolution (tens of picoseconds);
- compact size (the size of the sensitive SiPM area – 1 mm^2, 9 mm^2, 25 mm^2).

In the particular case, it is proposed to produce the collimator of lead or tungsten, including the connection circuit for gamma-probe for locating the source of ionizing radiation is: reed sensor; mechanical switch; sensor surface; infrared distance sensor.

The scheme of inclusion, represented by one of the above-mentioned methods, is necessary to activate the power supply circuit.

The current prototype gains these advantages using a 3x3 Hamamatsu silicon photomultipliers (SiPM) (Microsoft Point-to-Point Compression, MPPC) coupled to a 2x2x15mm LYSO scintillator. This enables energy resolution across a wide range of emitters, as well as high pulse rates (faster than a gas-tube device or avalanche photodiode (APD)).

The SiPM device itself is an array of 25-100 micron self-quenching APDs on a common substrate. Light from a scintillating medium triggers the avalanche of one (or multiple) cells, which creates a mV-scale electrical pulse lasting several hundred nanoseconds. The amplitude of such a pulse is proportional to the number of triggered APDs, and therefore proportional to the number of photons in the pulse of light incident on the SiPM plate. This allows direct correlation between the energy of the gamma rays hitting the scintillator and the amplitude of the pulses from the SiPM. Unlike the competition, this allows the device only to record the impact of gamma rays in a selected energy range if the user wishes.

Though extensive documentation exists regarding the modelling of various SiPMs, no manufacturer has made a SPICE (a free program for circuit simulations available from Linear Technologies) model available for researchers. However, it is not a difficult device to simulate. Since the SiPM is a massive array of avalanche photodiodes in parallel, it can be approximately modelled using passive components and a fast rise-time switch to simulate the momentary conduction of a triggered APD. As the physics of the avalanche process are outside of the scope of even the most advanced circuit simulation programs, this model is only approximate, and does not represent the

physics at work. As models of our type of MPPC have been constructed previously, we relied heavily on the work of Siefert et al. (2009) and Wangerin et al. (2008). The model itself was implemented in LTSPICE.

The model in Fig. 2, with limited modifications to adjust pulse height and shape, was used to simulate the amplifier input from the SiPM. To better reflect the behaviour of the real SiPM in the gamma-probe model, a small inductance was added in series with the SiPM output. Even with this addition, the raw SiPM output pulse-height is ~20% higher than the simulated value. Qualitatively, the pulse shape is nearly identical. This could be ascribed to a number of factors, but it is not significant enough to warrant further investigation.

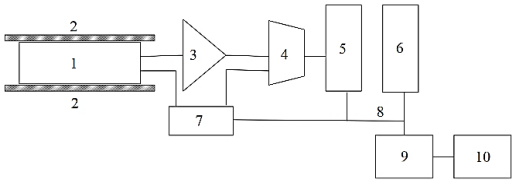

Figure 1: The general scheme of the gamma locator.

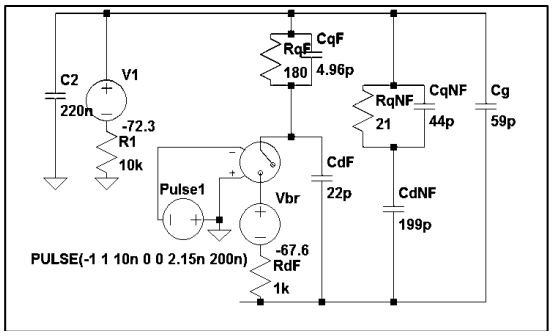

Figure 2: LTSpice implementation of the 3x3 MPPC model with values taken from Siefert et al. to reflect a pulse consisting of 2500/14400 cells firing.

Excluding the energy-resolution feature, the success of a device like the gamma-probe is determined by its angular selectivity, sensitivity and dynamic range. According to tests performed by A. Yagnyukova et al. (2015), the SiPM and crystal arrangement can achieve angular selectivity better than 26°, which is far better than existing devices.

Unfortunately, the device suffers from a high background count rate from the 1.19MeV decay of Lu-176 in the LYSO scintillator. Further limiting the dynamic range, scatter-background produced by the physical arrangement of the radioisotope within the patient can contribute significantly to noise. Gammas that traverse such a path, however, have necessarily lost energy through Compton scattering (Christillin 1986). The wavelength shift is given below in eqn. 1.

$$\lambda - \lambda' = \frac{h}{m_e c}(1 - \cos(\theta)), \qquad (1)$$

where λ is the initial wavelength; λ' is the wavelength after scattering; h is the Planck constant; m_e is the electron rest mass; c is the speed of light; θ is the scattering angle.

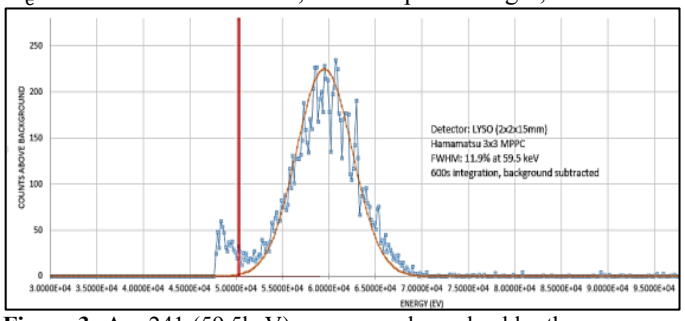

Figure 3: Am-241 (59.5keV) gamma peak resolved by the gamma-probe Mk.I detector with the Mk. II amplifier. Red line indicates the setting of the backscatter filter.

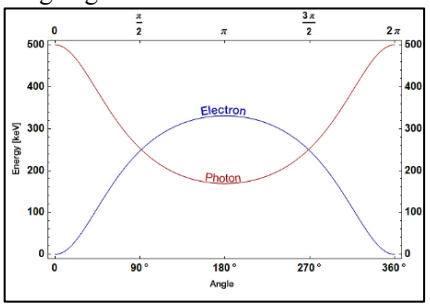

Figure 4: A plot of eqn. 1 in the energy domain for .5MeV photon (Compton scattering).

These Compton-scattered photons can be removed from the number of counts displayed using energy discrimination. By filtering large-angle or multiple scatters (with consummately large energy loss), the level of spurious counts can be reduced greatly.

The plot shows the energy of the scattered photon and the ejected electron versus the scattering angle.

The other advantages of the SiPM/LYSO system are achieved through the geometry of the scintillator/housing, as well as the use of a self-quenching device (as opposed to an active APD), which gives a higher maximum pulse-rate. Further, by using a RPP crystal with its longest dimension along the axis of the SiPM, proper collimating can be achieved without significant impact on the total mass or footprint of the scintillator/SiPM package.

3 MK. I device description

Specifications (see Fig. 5):

- Mass :<100g (no batteries)
- Power requirement: 80mA, 3.3V
- Angular selectivity[2]: 8º
- Sensor: Hamamatsu 3x3mm MPPC
- Scintillator: LYSO (Ce)
- Reflector: Lambertian
- Max count rate[2]: 1.3MHz
- Energy resolution[3]: 11.9%
- Noise floor[4]: ~40keV

This design functions as originally intended and registers radiation events. The USB interface serves as an effective tool for modifying device parameters, and the battery life is acceptable (>12h). Below are photos showing pulses from the SiPM in the presence of a radioisotope captured on a Teledyne LeCroy WaveAce 2024 oscilloscope.

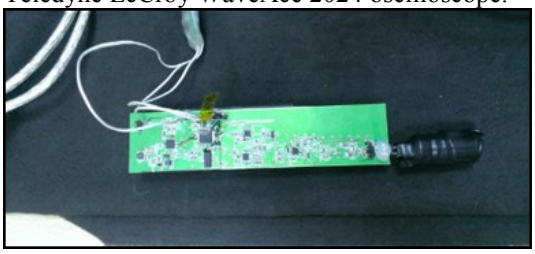

Figure 5: Mk.I board with SiPM/LYSO scintillator module installed (black canister on the right).

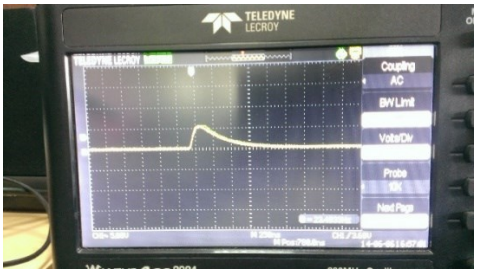

Figure 6: The trace is 1V/div (amp out).

Note the time interval is 250ns/div horizontally. This pulse is longer than ideal (~750ns), but the amplitude and shape are proper.

Amplifier impedance as a function of frequency. Generated with LTSPICE.

The Mk. I device is able to properly register pulses from the SiPM, but lacks pulse-height discrimination ability. As a result of higher-than-optimal gain the amplifier saturates, washing out all pulses larger than a fixed value. This causes obvious problems with energy resolution. Further, the SiPM is capable of pulses with $\tau < 100ns$ on the tail. However, in the recorded pulses above, $\tau > 500ns$. This limits the maximum pulse-rate to around 1.3MHz to avoid pile-up.

Note that R1 was later changed to 7.5k to reduce output-offset voltage.

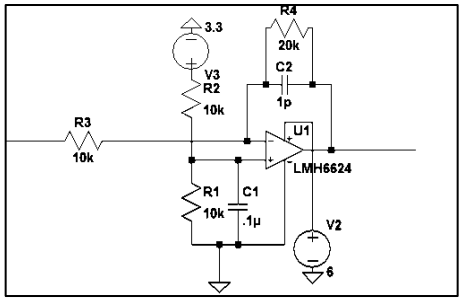

Figure 7: The amplifier design from the Mk. I prototype.

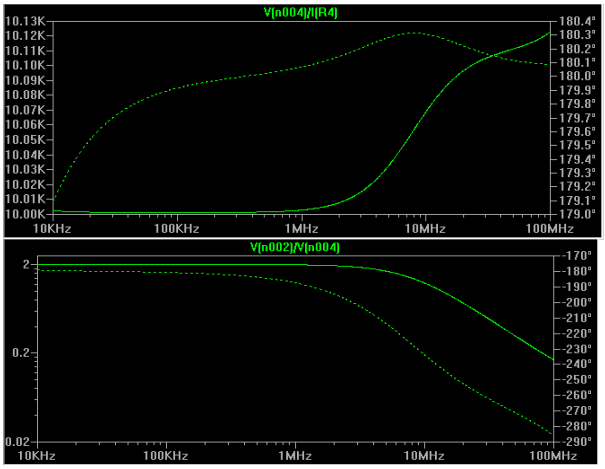

Figure 8: Amplifier gain as a function of frequency when DC gain is set to 2 (top).

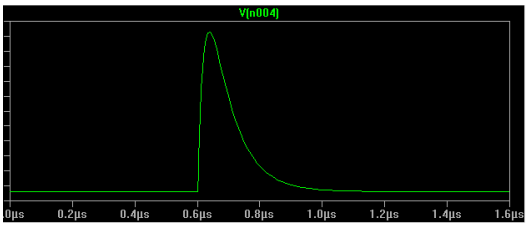

Figure 9: Amplifier output with simulated SiPM input pulse (see above).

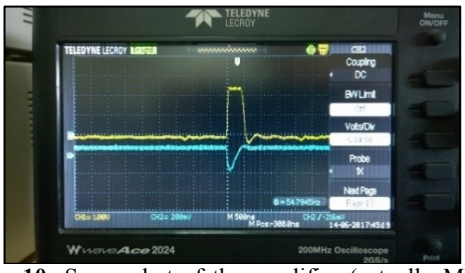

Figure 10: Scope shot of the amplifier (actually Mk. II) chopping pulses when the gain is set excessively high.

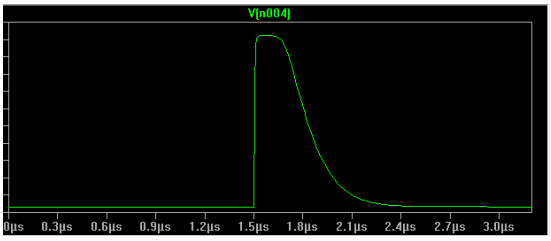

Figure 11: Image of LTSPICE simulated amplifier saturation in Mk. I amplifier (achieved by boosting the input signal amplitude).

Note that the time and amplitude settings are different from the first image, though the input pulses are near identical. This was the situation with the Mk. I design, but the extreme rarity (1/100 pulses) of saturation events made them hard to capture for an image.

4 MK. II amplifier development

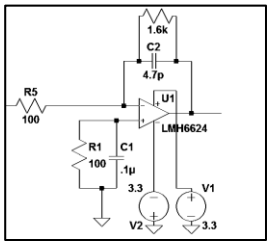

Figure 12: Mk. II amplifier design.

The development of the next version of the amplifier was informed by two ideas: to prevent signal chopping and to improve the recovery time of the amplifier. This was accomplished by building an amplifier circuit with a much lower input impedance, and with a full 0-3.3V range (Fig. 12). As in the previous section, all simulations were performed with LTSPICE.

The same IC (LMH6624) is used, though the LMH6629 has been suggested as a replacement.

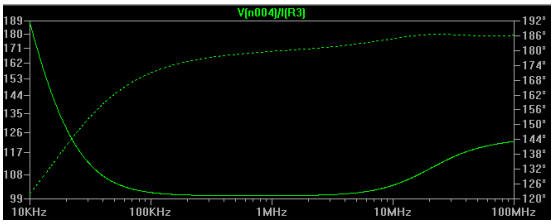

Figure 13: Amplifier Mk. II input impedance vs. signal frequency

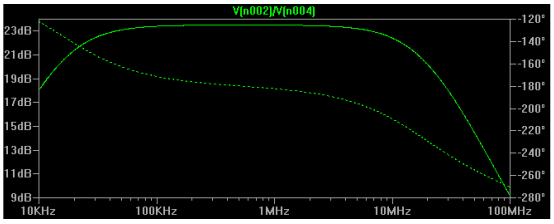

Figure 14: Amplifier gain as a function of signal frequency.

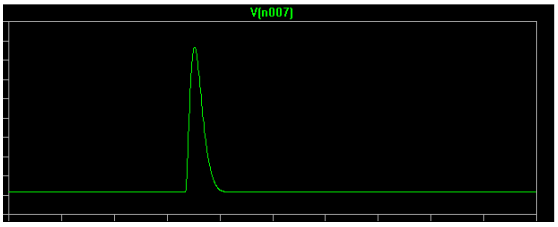

Figure 15: Sample output pulse from the amplifier.

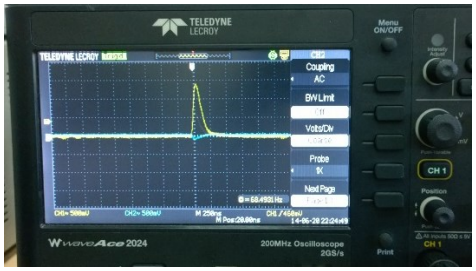

Figure 16: Input (blue) and output (yellow) pulses from the Mk. I SiPM and the Mk. II amplifier.

Note that this is roughly two orders of magnitude smaller than the Mk. I device.

This was conducted with an arbitrarily selected direct current gain of 18dB (the final value selected was 15dB).

However, this example pulse was significantly shorter than that observed in the test device, the Mk. II amplifier nonetheless made considerably shorter pulses (~200ns) than the Mk. I device (500-750ns). This discrepancy may be due to parasitic capacitance that went unaccounted for in the model.

Both are 500mV/div. The fall-time is ~200ns, and there is no saturation of the signal.

5 Testing and results

The next step after verifying that the amplifier was stable and not chopping pulse amplitudes was to gather a pulse-height spectrum from a known, minimally shielded gamma-emitter. Two sources were available, a Cs-137 source (~1uCi, 662keV) and an Am-241 source (~.1uCi, 59.5keV). Mk. II testing consisted of placing the samples as close to the end of the LYSO crystal as possible, then histogramming the pulse heights for 600s using a Teledyne LeCroy WaveRunner 620Zi. Background spectra were gathered in the same manner.

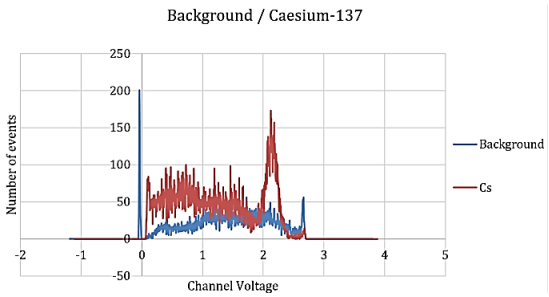

Figure 17: Cs-137 spectrum superimposed on a background count.

The raw spectra showed significant noise, especially at low energies. This was reduced using simple background subtraction.

The background peak at -0.045 was eliminated in the Cs spectrum because the trigger level was bumped up slightly.

After the measurements, background was subtracted out, but no smoothing was applied to the data. As usual, Gaussian peaks were fitted to the emitter peaks to measure resolution. The channel spacing was worked out using the known energies of the two emitters and the number of channels between

them. For this, the SiPM response and the LYSO energy-photon yield curve was assumed to be linear. The results are shown below.

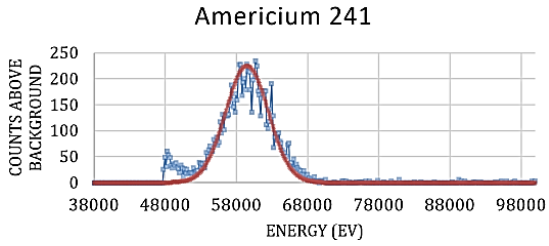

Figure 18: Americium-241 peak. 11.9% full width at half maximum (FWHM) at 59.5keV. 600s integration time from a 1uCi source.

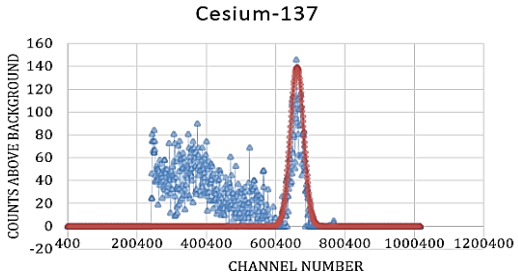

Figure 19: Cesium-137 peak, 7% FWHM from a 1uCi source (662keV).

Direct comparison of pulse-height histograms gathered from the amplifier input and output shows no significant distortion, excluding that related to the finite maximum pulse height. Lowering the gain of the amplifier could alleviate this problem, but at the cost of poorer channel spacing. This problem is a low-priority issue, however, because the targeted gamma-emitters are below 200keV characteristic energy, whereas the max pulse height exceeds 1MeV.

The resolution of the detectors is also within the range predicted by prior literature. This indicates proper function, but does not bode well for attempts to improve angular selectivity using scattering-angle. The energy loss for a Tc-99m photon (140keV) in a low angle scattering event (<60 degrees) is far less than can be resolved using this sensor. However, the energy-windowing approach should still be useful to filter out unwanted background from multiply scattered or highly attenuated photons.

6 Conclusion

The Mk. II amplifier shows considerably improved performance over the Mk. I device. However, quantitative measures of signal-to-noise ratio (SNR) and distortion have not been performed yet; preliminary tests show that the resolution and channel spacing of the detector are within reason. The noise floor (lowest channel below which dark counts dominate) appears to be around 40keV. This figure is yet again within reason, and indicates proper function of the SiPM and associated processing electronics. The detector resolution, while adequate for this size of crystal and sensor, does not appear to be high enough to be of use in trimming down angular selectivity. However, it is high enough so that effective background exclusion can be done.

Further testing using FLUKA (physical modelling) and LTSPICE (electrical modelling) should be carried out to optimize both the amplifier and the collimator. This could yield improvements in sensitivity, resolution and directionality. Further, these tests should be repeated with different scintillating media to determine the best crystal selection.

7 Acknowledgement

This work was supported by Competitiveness Growth Program of the Federal Autonomous Educational Institution of Higher Professional Education National Research Nuclear University MEPhI (Moscow Engineering Physics Institute).

References

Cancer. Fact sheet N°297. Updated February 2015. World Health Organization, 2015. URL: http://www.who.int/mediacentre/factsheets/fs297/en.

Blokhin N.N., Peterson B.B. Clinical oncology, M., 1979.

World Cancer Report 2014. Edited by Bernard Stewart and Christopher P. Wild. IARC Nonserial Publication, 2014. 630 pages.

De Martel C, Ferlay J, Franceschi S, et al. Global burden of cancers attributable to infections in 2008: a review and synthetic analysis. The Lancet Oncology 2012;13. Pages 607-615.

Zubovsky G.A. Gammascintigraph, M., 1978.

Clinical Radiology, ed. Zedgenidze G.A., v. 4, Moscow, 1985.

Gamma Probes. IntraMedical Imaging, 2014. URL: http://www.gammaprobe.com/products/gamma-probes.

Wengenmair H., Kopp J. Gamma Probes for Sentinel Lymph Node Localization: Quality Criteria, Minimal Requirements and Quality of Commercially Available Systems. 2005. URL: http://www.klinikum-augsburg.de/index.php/fuseaction/download/lrn_file/gammaprobes.pdf.

Da Costa, F.E.; Rela, P.R.; de Oliveira, I.B.; Pereira, M.C.C.; Hamada, M.M. Surgical gamma probe with TlBr semiconductor for identification of sentinel lymph node. IEEE Nuclear Science Symposium Conference Record, 2005. Pages: 2890 – 2894.

Wei, L., Chen, F., Zhang, X., Li, D., Yao, Z., Deng, L., Xiao, G. 99mTc-dextran lymphoscintigraphy can detect sentinel lymph node in breast cancer patients. Experimental and Therapeutic Medicine, Volume 9, Issue 1, 1 January 2015. Pages 112-116.

Bogliolo, S., Marchiole, P., Sala, P., Giardina, E., Villa, G., Fulcheri, E., Menada, M.V. Sentinel node mapping with radiotracer alone in vulvar cancer: A five year single-centre experience and literature review. European Journal of Gynaecological Oncology, Vol 36, Issue 1, 2015. Pages 10-15.

Endo, K., Ueno, T., Tsuji, A., Kondo, S., Wakisaka, N., Murono, S., Yoshizaki, T. Sentinel node biopsy and tumor-targeted chemotherapy for oral squamous cell carcinoma. Oto-Rhino-Laryngology Tokyo, Volume 56, Issue 5, October 2014. Pages 329-331.

Matheoud, R., Giorgione, R., Valzano, S., Sacchetti, G., Colombo, E., Brambilla, M. Minimum acceptable sensitivity of intraoperative gamma probes used for sentinel lymph node detection in melanoma patients. Physica Medica, 30(7), 2014. Pages 822-826.

Grigorenko A., Panfilov L., Smirnov A., Starikovskiy A., Rubin D., Shulga E., Sychev N., Nikolaeva A.. The existing gamma-probes review for searching functional increase and complex improvement possibilities. Biosciences Biotechnology Research Asia, 2015. Vol. 12, p. 197-200.

G.N. Lebedev, A.K. Yagnyukova, A.M. Tolstaya, I.G. Bulychev. Gamma-Probe Based on Scintillation Crystal and Silicon Photomultipliers for Cancer Detection. International Journal of Tomography and Simulation, Volume 29, Issue Number 3, 2016. Pages: 92-103.

Romanova S. 'Nuclear medicine: status and prospects'. Remedium, 2013, No. 6. Pages 8-20.

Georgiou, M. Evaluation of an imaging gamma probe based on R8900U-00-C12 PSPMT. IEEE Nuclear Science Symposium and Medical Imaging Conference, 2011. Pages: 4020 – 4023.

Seifert, S.; van Dam, H.T.; Huizenga, J.; Vinke, R.; Dendooven, P.; Lohner, H.; Schaart, D.R. Simulation of Silicon Photomultiplier Signals. IEEE Transactions on Nuclear Science, 56(6), 2009. Pp 3726 – 3733.

Wangerin, K.A.; Gin-Chung Wang; Kim, Chang; Danon, Yaron. Passive electrical model of silicon photomultipliers. IEEE Nuclear Science Symposium Conference Record, 2008, 4906 – 4913.

P. Christillin. Nuclear Compton scattering. J. Phys. G: Nucl. Phys. 12 (9), 1986. Pages: 837 – 851.

Anastasia Yagnyukova, Dmitry Mikhaylov, Timur Khabibullin, Andrey Grigorenko, Panfilov Leonid. Gamma-Probe for Revealing Cancerous Cells. Studies on Ethno-Medicine, 2015.

Compton scattering. URL: http://en.academic.ru/dic.nsf/enwiki/35148.